applied sciences

MDPI

Article

Beam Control in an Intracavity Frequency-Doubling Semiconductor Disk Laser

Guanyu Hou [1,2], Lijie Wang [1], Jian Feng [1,2], Andreas Popp [3], Berthold Schmidt [3], Huanyu Lu [1,2], Shili Shu [1], Sicong Tian [1], Cunzhu Tong [1,*] and Lijun Wang [1]

1 State Key laboratory of Luminescence and Applications, Changchun Institute of Optics, Fine Mechanics and Physics, Chinese Academy of Sciences, Changchun 130033, China; jumjim88@126.com (G.H.); wanglijie@ciomp.ac.cn (L.W.); fengjian12453@163.com (J.F.); 18744019056@163.com (H.L.); shushili@ciomp.ac.cn (S.S.); tiansicong@ciomp.ac.cn (S.T.); wanglijun@ciomp.ac.cn (L.W.)

2 Center of Materials Science and Optoelectronics Engineering, University of Chinese Academy of Sciences, Beijing 100049, China

3 TRUMPF GmbH, 71254 Ditzingen, Germany; Andreas.Popp@trumpf.com (A.P.); berthold.schmidt@trumpf.com (B.S.)

* Correspondence: tongcz@ciomp.ac.cn

Received: 23 February 2019; Accepted: 9 April 2019; Published: 17 April 2019

Abstract: In this paper, we have demonstrated a 1.3 W green laser using a V-shaped intracavity frequency doubling 1036 nm semiconductor disk laser. The beam quality of the fundamental and second harmonic generation (SHG) laser is investigated. It has been found that the output lasers at the fundamental and SHG wavelength both suffer from reduced beam quality along with power scaling. The measured beam profile is elliptical under high power operation. In order to improve the SHG laser beam, an intracavity aperture is employed to control the mode characteristics of fundamental frequency light. By fine-tuning the aperture, a nearly circular beam profile with improving beam quality and brightness is realized.

Keywords: semiconductor disk laser; frequency doubling; beam control; beam quality

1. Introduction

High brightness green lasers are attractive for a wide range of applications, such as laser displays, biophotonics, underwater laser communication, and pump sources for Ti:Sapphire lasers. There are two main techniques used to attain green laser emission presently. The first one is GaN-based diode laser that directly emits in the green spectral range [1–4]. Although the green diode laser has made great strides in its power, efficiency and spectral coverage, it is still hard to achieve watt-class continuous power with high beam quality. The second approach is based on non-linear frequency conversion including frequency double or sum-frequency generation of lasers emitting in the near-infrared range. Traditionally, frequency-doubled diode pumped solid state lasers show high output power with excellent beam properties. However, they can only emit light in a discrete set of wavelengths dependent on certain fixed atomic transitions, limiting the widespread adoption of intended applications [5]. Using a semiconductor gain medium instead of solid crystals, optically pumped semiconductor disk lasers (OP-SDL) show promising advantages of wavelength flexibility, power scalability and good beam quality. Their ability to insert a frequency doubling crystal in the resonator cavity allows the generation of a green laser beam, whose wavelength can be fine tailored around the desired wavelength by engineering the composition of semiconductor materials. By employing the intracavity frequency doubling, many green SDLs with various wavelengths have been demonstrated, such as 62 mW at

501 nm [6], 100 mW at 505 nm [7], 0.7 W at 520 nm [8], 220 mW at 529 nm [9], 20 W at 532 nm [10] and 7 W at 535 nm [11].

Another advantage of SDL, inherited from optically pumped solid-state lasers, is that its free-space cavity configuration allows for the convenient insertion of additional optical elements, such as a birefringent filter for single-frequency output [12], an etalon for two-color emission [13], or an intracavity aperture for mode locking [14]. In most SDL systems, power scaling is achieved by simply increasing the beam size and pumped area on the gain chip. Such a high power operation may be realized at a price of relative low beam quality due to large spot size [15], even though the external cavity of SDL plays a role of transverse mode selection. The beam shape and beam quality of fundamental frequency light have an important influence on the second harmonic generation (SHG). Also, the temperature rise of SHG materials as a function of the power and focusing conditions may cause a thermal dephasing and thermal lensing effect, deteriorating the beam quality of the SHG light. Therefore, an extra beam control element may be required to achieve certain beam behavior. Some previous works have inserted mode-control element into the cavity of SDLs for generating spatially structured beams, like higher-order modes [16]. However, utilizing the beam control element to improve the beam quality and profile was rarely reported.

In this paper, we demonstrated a 1.3 W green laser using a V-shaped intracavity frequency doubling SDL. The output lasers at the fundamental and SHG wavelength both suffer from reduced beam quality under high power operation. Therefore, an aperture is employed without changing cavity configuration for controlling the mode characteristics of SHG. The dependence of output power, beam quality and beam profile on the aperture size are investigated. At an optimized condition, the brightness of green laser is improved and a near circular beam profile is obtained.

2. Semiconductor Disk Laser (SDL) Design and Bonding Process

Figure 1 shows the SDL chip structure in our experiment. The wafer was grown by metal-organic vapor phase epitaxy (MOVPE) in a reverse order on a GaAs substrate. It consists of three sections: a highly reflective distributed Bragg reflector (DBR) mirror, a gain region and a cap layer. The DBR mirror is made up of 20 pairs of alternating AlAs/GaAs layers, and each layer has an optical thickness equivalent to a quarter of the designed lasing wavelength. The active region includes 10 layers of 8 nm InGaAs compressively strained quantum wells (QWs) with GaAs barrier and a tensile strained GaAsP layer for strain compensation. Those QWs are distributed periodically at the anti-nodes of the optical standing wave in the micro-cavity formed between the DBR and the cap layer [17]. A large energy bandgap InGaP cap layer with an optical thickness of a half wavelength is utilized to confine the excited carriers in the gain region in order to prevent the surface recombination [18]. Furthermore, the InGaP cap is transparent for both of the pump light and the emission laser. In this paper, the SDL is designed to emit at around 1021–1045 nm, and the active region is optimized for efficient optically pumping in the wavelength range of 790–820 nm.

Efficient thermal management is crucial for high power operation of SDLs. In order to enhance the heat dissipation in the SDL, we use a pre-metallization method of the diamond-semiconductor chip bonding process [19]. A 5 × 5 × 1.2 mm diamond deposited by chemical vapor deposition (CVD) is used as the heat-spreader. The SDL size is 3 mm × 3 mm. Figure 2 shows the detail of the SDL bonding structure. The pre-metallization of diamond is performed by depositing Cu-Sn alloy (Sn component: 5–7%) on both the top and bottom surfaces of the diamond. The thickness of the pre-metalized layer on the diamond surface is 100 nm. Then Ti/Pt/Au layers are also deposited on both sides of the pre-metalized diamond and the DBR side of the SDL chip. After that, the chip is bonded on the diamond using indium. In order to dissipate the heat efficiently, the diamond is bonded on a large copper heatsink using indium. Finally, the GaAs substrate is removed by selective wet etching. A thermoelectric cooler (TEC) is mounded underneath the copper heatsink to control the temperature of SDLs.

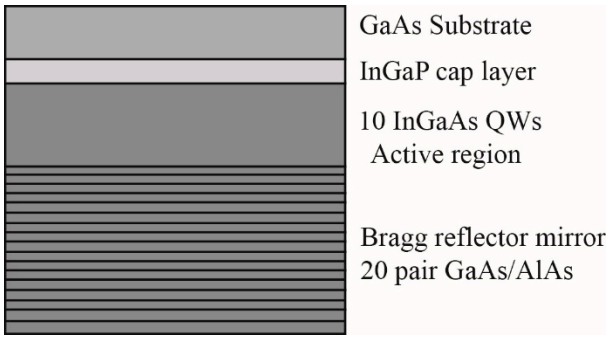

Figure 1. Schematic diagram of the designed semiconductor disk laser (SDL).

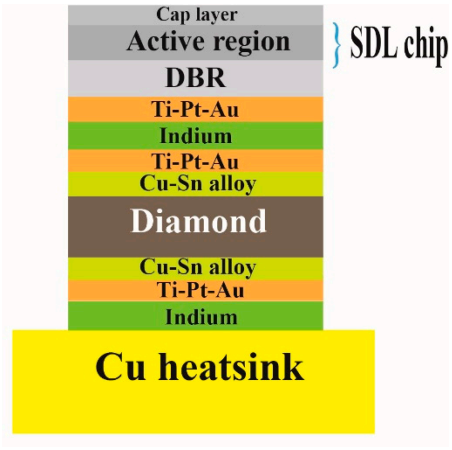

Figure 2. Schematic diagram of the bonding structure.

3. Experimental Results and Discussion

A standard V-shaped laser cavity configuration is used in our experiment as shown in Figure 3, which is formed by the semiconductor's DBR as one end mirror, a curved folding mirror (M1) and a planar mirror (M2). The mirror M1 is highly reflective (HR) at 1030 nm but highly transmissible for the second-harmonic wavelength of 515 nm, which has a curvature radius of 250 mm and is placed at a distance of 345 mm from the SDL chip. The measured reflectivity of M1 is $R > 99.8\%$ from 650 nm to 1100 nm and $R < 5\%$ from 488 nm to 532 nm. In order to form the resonator, M1 has a tilting angle of about 9° related to the axis of the SDL. Before inserting the SHG crystal, the output power at the fundamental wavelength was measured at the followed situation. A plane mirror was used as M2 mirror with a 3% transmission for the fundamental wavelength of around 1030 nm, and plays a role of output coupler. Then the output power of SDL was measured and shown in Figure 4. The TEC temperature was set as 13 °C, and the temperature of cooling water is 12 °C. The pump beam of 808 nm diode laser was incident at 40° angle relative to the surface normal and was focused on the SDL chip with a spot diameter of 300 μm. This angle produced an elliptical pump spot, which may not only reduce the pumping efficiency compared with nearly circular beam shape [20], but also degrade the beam quality. The continuous wave (CW) output power is over 3.5 W under 25 W pump power. As about 30% of the pump power was reflected on the un-coated SDL surface, the optical-to-optical efficiency related to the absorbed pump power is about 20%. No thermal rollover occurred within the available range of pump powers, indicating the efficient heat dissipation of our packaged method.

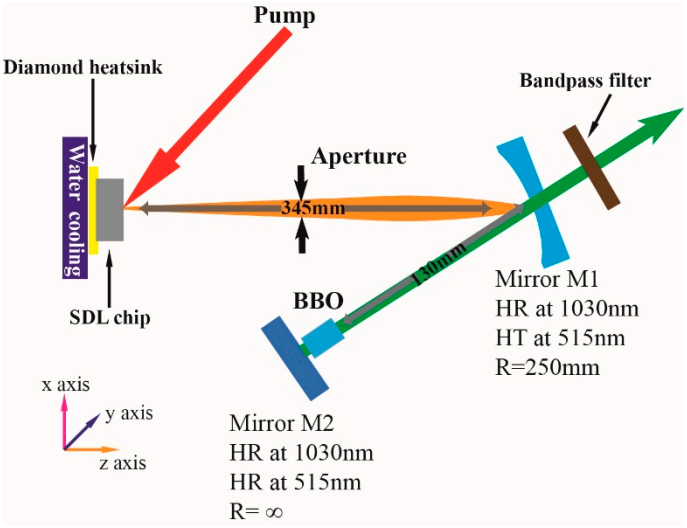

Figure 3. Schematic of the V-shaped resonator for green laser.

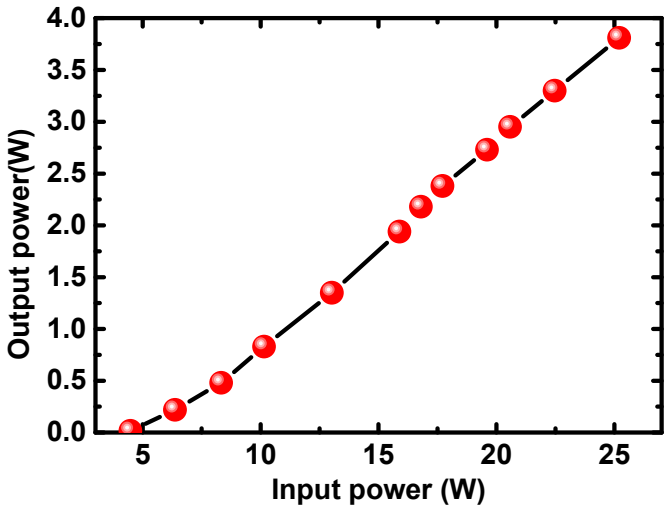

Figure 4. Output power at 1036 nm as a function of the 808 nm pump power.

For the SHG experiment, we replace the plane output coupler described as above with a plane end mirror M2. This mirror M2 is highly reflective for both the fundamental and the second-harmonic laser. The pump laser and the spot size are not changed. The mode diameter on the SDL is about 500 µm. M2 is located at the position of the beam waist, which is 130 mm far from M1 and has a spot size around 80 µm. To produce a green laser beam, a 3 mm long beta-barium borate (BBO) crystal is inserted near to the mirror M2, which is coated with moisture-proof antireflection film on both sides. The full experimental setup is schematically shown in Figure 3.

Figure 5 shows the lasing spectra of the 1036 nm fundamental wave and the green light at 516 nm, which are measured with a fiber-coupled spectrometer. The linewidths of the fundamental and frequency-doubling laser defined as the full-width at half-maximum (FWHM) of lasing spectra are 4.5 nm and 1.5 nm, respectively. In this experiment, we do not use the birefringent filter in order to reduce the power loss, but the wide spectral width of the fundamental laser will sacrifice the conversion efficiency.

The CW output characteristic of green laser is shown in Figure 6. The TEC temperature was set to 13 °C. The pump threshold is about 6 W, and the slope efficiency is 9.4% for the frequency-doubling generation. The maximum output power is 1.3 W under the input power of 25 W, corresponding to the maximum optical to optical conversion efficiency is 6.3%. Also, this corresponds to a frequency conversion efficiency of 27% with respect to the maximum fundamental power.

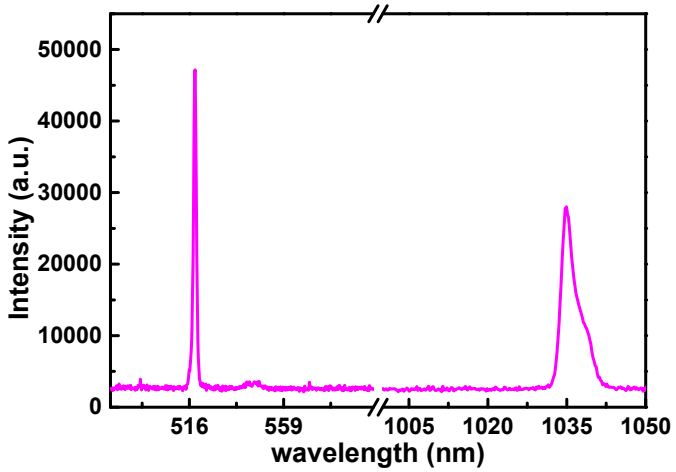

Figure 5. Spectrum of the fundamental and green SDL.

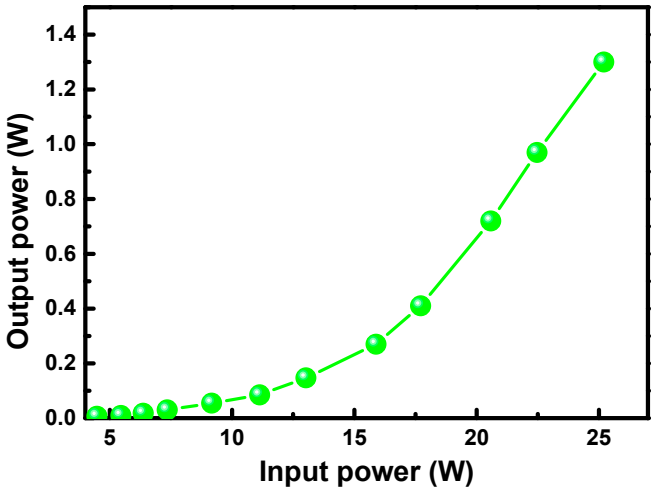

Figure 6. Output powers of the green SDL.

We also investigated the beam quality M^2 of the fundamental and the green laser respectively. The M^2 factors were measured by a commercial beam propagation analyzer M2MS-BP209 according to the ISO11146 standard. Figure 7 illustrates the beam quality of the fundamental frequency laser under various input powers from 6 W to 25 W. It can be seen that the value of M_x^2 (the black) is in the range from 2.70 to 3.65. By contrast, the M_y^2 (the red) is much better, which varies from 1.35 to 1.62. The measured spot shows that the fundamental laser beam is not perfectly circular but elliptical as shown in the inset of Figure 7. At higher input power, fluctuation appears in the M^2 curve, which may be resulted from the completion of high-order modes.

The beam quality of the green laser is represented in Figure 8. At the input power lower than 18 W, M_x^2 is slightly better than M_y^2, which is below 4.0 in this range. The lowest value of M_x^2 is nearly 2. The values of M_y^2 are around 3.4, and they are not sensitive to the input power. At higher input power, the beam quality becomes unstable especially for M_x^2. So we measured the M^2 value multiple times for each input power, and the error bar is shown in Figure 8. For M_x^2, the average value increases dramatically from 2.20 to 7.61 with the input power variating from 16 W to 25 W. The error enlarges with increasing input power, which is more likely due to more high-order mode generation and a correspondingly more unstable cavity. It is related to the beam quality fluctuations of the fundamental frequency laser as mentioned in Figure 7. In contrast, it is quite different for M_y^2 at higher input power. Even though the error of M_y^2 is larger than that at lower input power, but the error range is much lower

than that of M_x^2. The M_y^2 is in the range from 2.0 to 3.6. It seems that the y-axis is much more stable than the x-axis, which is insensitive to input power.

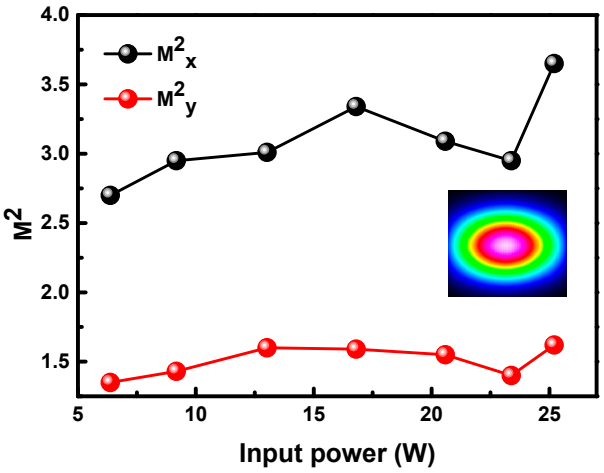

Figure 7. Beam quality M^2 factors of the fundamental laser in x and y directions. The inset is the beam profile at input power of 25 W.

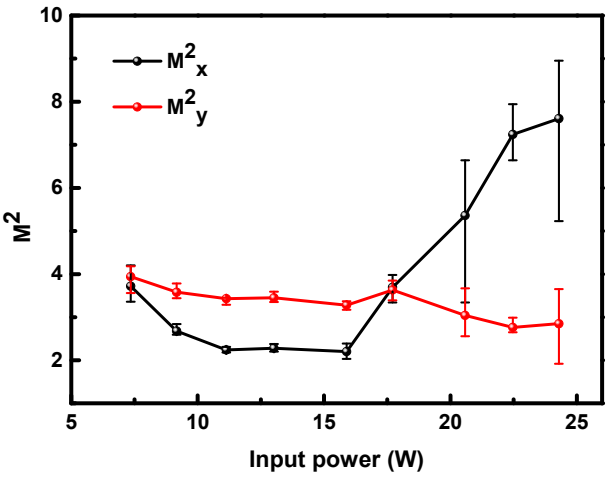

Figure 8. Beam quality M^2 factors of the green laser in x and y directions.

In order to improve the beam quality of the green laser under a high power operation, we introduce a simple aperture into the V-shaped cavity which is shown in Figure 3. The aperture is located between the SDL chip and M1, and the distance from the SDL is about 150 mm. Figure 9 shows the measured beam quality at input power of 25 W with different diameter sizes D of the aperture. The insets in Figure 9 are the beam profiles and the aperture used in this experiment. For this given power, the beam quality measurement starts from the diameter size of 1.5 mm. When reducing the aperture size, the values of the M_x^2 and M_y^2 slightly decline. However, when the aperture narrows to D < 1.0 mm, the M_x^2 and M_y^2 drop dramatically to approximate 1.5 at D = 0.8 mm (the smallest size of this aperture). The beam quality gets better both in x and y axis, and especially M_x^2 exhibits a three- to four-fold improvement. Furthermore, the beam profile changes from ellipse to near circular shape shown in the inset of Figure 9. In such a V-shape laser cavity, the distances between the SDL chip and the mirrors should be carefully chosen for effective transverse mode selection. However, the optimal conditions can only be valid for a certain pump power range, increasing the difficulty in the design. In this paper, we utilize an aperture to control the beam size of the fundamental laser without changing the cavity configuration. Through this experiment, some important parameters like the optical pump

size can be determined to ensure fundamental mode operation, which could ensure mode matching and appropriate focusing into the non-linear crystal.

We also investigate the dependences of output power and beam brightness on the aperture size. It can be seen from Figure 10 that the output power decreases with narrowed D, which accords with our expectations as a reason for more light blocked by this aperture. The other parameter for assessing the performance of the green lasers is the brightness B, which is defined as [21]:

$$B = \frac{P}{\lambda^2 M_x^2 M_y^2} \quad (1)$$

where P is the output power, λ is the center wavelength. As shown in Figure 10, when D > 1 mm, the brightness decreases along with the output power dropping. Even though the brightness B error is large at higher power, the biggest B is still below 30 $MWcm^{-2}sr^{-1}$ and the average values are in the range from 12 to 25 $MWcm^{-2}sr^{-1}$. When D < 1.0 mm, the brightness increases to above 30 $MWcm^{-2}sr^{-1}$ and reaches the maximum of 35 $MWcm^{-2}sr^{-1}$. Finally, at this aperture size, we achieve a near circular profile, quiet good beam quality and high brightness green beam.

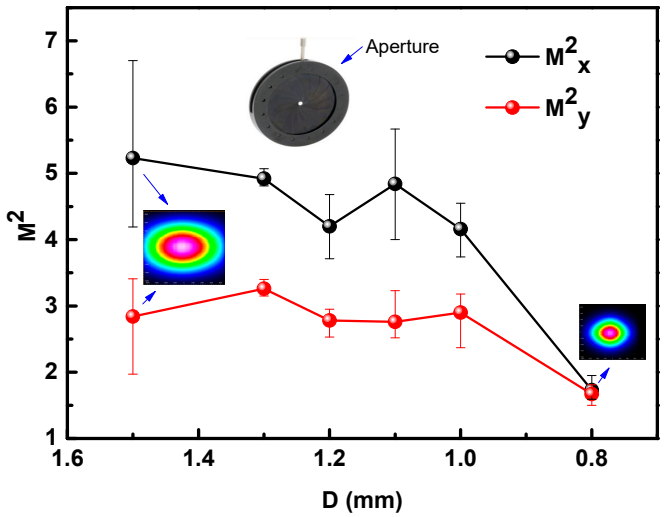

Figure 9. Dependences of the beam quality M^2 factors of the green laser in x and y directions on the aperture diameter size D at 25 W input power. The inset is the green beam profile at D = 1.5 mm and 0.8 mm, and with the aperture used in this experiment.

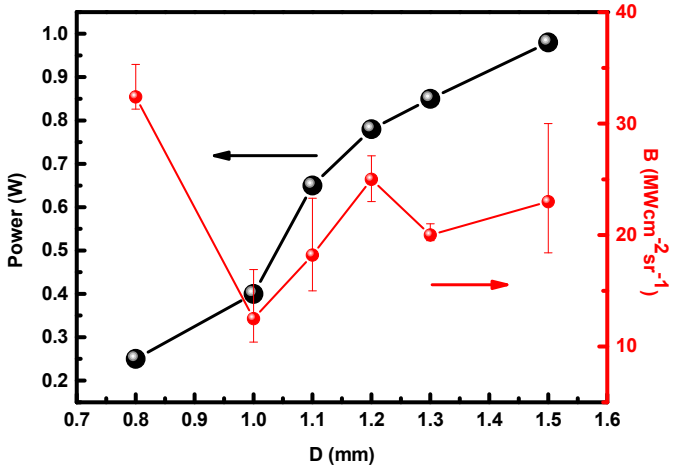

Figure 10. Dependences of output power and beam brightness on the aperture size D at 25 W input power.

4. Conclusions

In summary, we have demonstrated an intracavity frequency-doubled 516 nm green SDL using a type I phase-matched BBO as the non-linear crystal. The maximum output power is 1.3 W corresponding to a conversion efficiency of 27% with respect to the maximum fundamental power. The beam quality of the fundamental and SHG laser is investigated. By inserting an additional aperture in the laser cavity, we study the influence of the aperture size on the beam quality and beam profile of the output green laser. Finally, a nearly circular beam profile is realized with improved beam quality and brightness. This can provide a clear guide of how to further optimize the pump spot size and the distances for single fundamental mode operation.

Author Contributions: Data curation, G.H. and J.F.; Formal analysis, S.S. and S.T.; Funding acquisition, A.P. and B.S.; Investigation, G.H.; Supervision, C.T. and L.W. (Lijun Wang); Validation, L.W. (Lijie Wang) and H.L.; Writing—original draft, G.H.; Writing—review & editing, L.W. (Lijie Wang).

Funding: This work was supported by TRUMPF GmbH, in part by National Natural Science Foundation of China (Nos. 61790584, 61761136009 and 61774153).

Conflicts of Interest: The authors declare no conflict of interest.

References

1. Weng, G.; Mei, Y.; Liu, J.; Hofmann, W.; Ying, L.; Zhang, J.; Bu, Y.; Li, Z.; Yang, H.; Zhang, B. Low threshold continuous-wave lasing of yellow-green InGaN-QD vertical-cavity surface-emitting lasers. *Opt. Express* **2016**, *24*, 15546–15553. [CrossRef] [PubMed]
2. Miyoshi, T.; Masui, S.; Okada, T.; Yanamoto, T.; Kozaki, T.; Nagahama, S.; Mukai, T. 510–515 nm InGaN-Based Green Laser Diodes onc-Plane GaN Substrate. *Appl. Phys. Express* **2009**, *2*, 062201. [CrossRef]
3. Enya, Y.; Yoshizumi, Y.; Kyono, T.; Akita, K.; Ueno, M.; Adachi, M.; Sumitomo, T.; Tokuyama, S.; Ikegami, T.; Katayama, K.; et al. 531 nm green lasing of InGaN based laser diodes on semi-polar {2021} free-standing GaN substrates. *Appl. Phys. Express* **2009**, *2*, 082101. [CrossRef]
4. Kasahara, D.; Morita, D.; Kosugi, T.; Nakagawa, K.; Kawamata, J.; Higuchi, Y.; Matsumura, H.; Mukai, T. Demonstration of Blue and Green GaN-Based Vertical-Cavity Surface-Emitting Lasers by Current Injection at Room Temperature. *Appl. Phys. Express* **2011**, *4*, 072103. [CrossRef]
5. Bai, J.; Chen, G. Continuous-wave diode-laser end-pumped Nd:YVO 4 /KTP high-power solid-state green laser. *Opt. Laser Technol.* **2002**, *34*, 333–336. [CrossRef]
6. Jacquemet, M.; Domenech, M.; Lucas-Leclin, G.; Georges, P.; Dion, J.; Strassner, M.; Sagnes, I.; Garnache, A. Single-frequency cw vertical external cavity surface emitting semiconductor laser at 1003 nm and 501 nm by intracavity frequency doubling. *Appl. Phys. B* **2006**, *86*, 503–510. [CrossRef]
7. Seelert, W.; Kubasiak, S.; Negendank, J.; Elm, R.V.; Chilla, J.; Zhou, H.; Weiss, E. Optically-pumped semiconductor lasers at 505-nm in the power range above 100 mW. *Proc. SPIE* **2006**, *6100*, 610002. [CrossRef]
8. Lutgen, S.; Kuehnelt, M.; Steegmueller, U.; Brick, P.; Albrecht, T.; Reill, W.; Luft, J.; Kunert, B.; Reinhard, S.; Volz, K. Green semiconductor disk laser with 0.7 W cw output power. *Proc. SPIE* **2005**, *5737*, 109–113. [CrossRef]
9. Hartke, R.; Heumann, E.; Huber, G.; Kühnelt, M.; Steegmüller, U. Efficient green generation bintracavity frequency doubling of an optically pumped semiconductor disk laser. *Appl. Phys. B* **2007**, *87*, 95–99. [CrossRef]
10. Tropper, A.C.; Berger, J.D.; Anthon, D.W.; Caprara, A.; Chilla, J.L.; Govorkov, S.V.; Lepert, A.Y.; Mefferd, W.; Shu, Q.Z.; Spinelli, L. 20 Watt CW TEM00 intracavity doubled optically pumped semiconductor laser at 532 nm. *Proc. SPIE* **2012**, *8242*, 824206. [CrossRef]
11. Lee, J.; Lee, S.; Kim, T.; Park, Y. 7 W high-efficiency continuous-wave green light generation by intracavity frequency doubling of an end-pumped vertical external-cavity surface emitting semiconductor laser. *Appl. Phys. Lett.* **2006**, *89*, 241107. [CrossRef]
12. Zhang, F.; Heinen, B.; Wichmann, M.; Moller, C.; Kunert, B.; Rahimi-Iman, A.; Stolz, W.; Koch, M. A 23-watt single-frequency vertical-external-cavity surface-emitting laser. *Opt. Express* **2014**, *22*, 12817–12822. [CrossRef] [PubMed]

13. Matthias, W.; Mohammad Khaled, S.; Fan, Z.; Bernd, H.; Maik, S.; Arash, R.I.; Wolfgang, S.; Moloney, J.V.; Koch, S.W.; Martin, K. Evolution of multi-mode operation in vertical-external-cavity surface-emitting lasers. *Opt. Express* **2013**, *21*, 31940–31950. [CrossRef]
14. Gaafar, M.; Moller, C.; Wichmann, M.; Heinen, B.; Kunert, B.; Rahimi-Iman, A.; Stolz, W.; Koch, M. Harmonic self-mode-locking of optically pumped semiconductor disc laser. *Electron. Lett.* **2014**, *50*, 542–543. [CrossRef]
15. Chilla, J.L.A.; Butterworth, S.D.; Zeitschel, A.; Charles, J.P.; Caprara, A.L.; Reed, M.K.; Spinelli, L. High power optically pumped semiconductor lasers. *Proc. SPIE* **2004**, *5332*, 143–151. [CrossRef]
16. Lukowski, M.L.; Meyer, J.T.; Hessenius, C.; Wright, E.M.; Fallahi, M. Generation of high-power spatially structured beams using vertical external cavity surface emitting lasers. *Opt. Express* **2017**, *25*, 25504–25514. [CrossRef] [PubMed]
17. Laurain, A.; Myara, M.; Beaudoin, G.; Sagnes, I.; Garnache, A. Multiwatt-power highly-coherent compact single-frequency tunable vertical-external-cavity-surface-emitting-semiconductor-laser. *Opt. Express* **2010**, *18*, 14627–14636. [CrossRef] [PubMed]
18. Mueller, M.; Linder, N.; Karnutsch, C.; Schmid, W.; Streubel, K.P.; Luft, J.; Beyertt, S.S.; Giesen, A.; Doehler, G.H. Optically pumped semiconductor thin-disk laser with external cavity operating at 660 nm. *Proc. SPIE* **2002**, *4649*, 265–272. [CrossRef]
19. Hou, G.Y.; Shu, S.; Feng, J.; Andreas, P.; Berthold, S.; Lu, H.Y.; Wang, L.J.; Tian, S.C.; Tong, C.Z.; Wang, L.J. High power (>27 W) semiconductor disk laser based on pre-metallized diamond heat-spreader. *IEEE Photonics J.* **2019**, in press.
20. Kim, G.B.; Kim, J.Y.; Lee, J.; Yoo, J.; Kim, K.-S.; Lee, S.-M.; Cho, S.; Lim, S.J.; Kim, T.; Park, Y. End-pumped green and blue vertical external cavity surface emitting laser devices. *Appl. Phys. Lett.* **2006**, *89*, 181106. [CrossRef]
21. Diehl, R.D.; Diehl, R.L. *High-Power Diode Lasers: Fundamentals, Technology, Applications*; Springer: Berlin/Heidelberg, Germany, 2000.